Fracture Mechanics of Concrete and Concrete Structures -
Assessment, Durability, Monitoring and Retrofitting of Concrete Structures- B. H. Oh, et al. (eds)
© 2010 Korea Concrete Institute, Seoul, ISBN 978-89-5708-181-5

Analysis of balanced double-lap joints with a bi-linear softening adhesive

C. S. Hansen & H. Stang
Department of Civil Engineering, Technical University of Denmark, Kgs. Lyngby, Denmark

J. W. Schmidt
Department of Civil Engineering, Technical University of Denmark, Kgs. Lyngby, Denmark COWI A/S, 2800 Kgs. Lyngby, Denmark

ABSTRACT: The response of a bonded symmetric balanced double lap joint under tensile loading with a bi-linear softening adhesive is described with a closed form solution. Since bonded joints in concrete structures undergo softening, a versatile model to describe the response for a wide range of constitutive relationships is needed. A constitutive relationship containing a bi-linear softening law contains such versatility. The solution was investigated for moderate and extreme softening parameters. The solution for extreme softening parameters, exhibited a non-physical behavior, where the size of the stress-free crack decreased for increasing size of fracture process zone. This suggests that in order to fully describe the loading and unloading response, an unloading law should be implemented in the constitutive model. Apart from adhesively bonded metallic joints, the present solution may be used in analysis of cracked concrete disks strengthened with adhesive bonded fiber reinforced polymers (FRP), or in any other structure comparable to a double lap joint with a softening interface. The present constitutive model can be changed to fit any model with the same shape of constitutive relationship, see Figure 1.

1 INTRODUCTION

1.1 *General*

Since bonded lap joints in concrete structures often exhibit softening behavior, the prediction of the response relies on the ability to model the softening in a constitutive law. In an analysis of FRP or steel bonded to a concrete surface, the typical softening law used is linear. Such a model rule out modeling of more complex softening branches obtained from tests. This could be exponential softening, sudden drops or ductile softening behavior. The ability to analyze the behavior of bi-linear softening adhesives in joints is important, since a simple bi-linear behavior can be used as approximation for complicated softening behavior experienced in tests. With a bi-linear softening relationship, it is possible to approximate both convex and concave descending softening branches. This paper analyzes a symmetric balanced double lap joint with a bi-linear softening adhesive using a simple joint theory, first described in Volkersen (1938). Volkersen assumed linear elastic materials, adhesive loaded and deformed in shear only and adherents allowing only axial deformation. Extensions to Volkersens model such as softening and hardening behavior have been proposed since, and a vast amount of work on stress analysis and bond and anchorage models exist based upon it. See as examples, Hart-Smith (1973), Ranisch (1982), Gustafsson (1987), Pichler (1993), Täljsten (1995), Chen & Teng (2001), Yuan et al. (2004). Many of these papers make use of a cohesive law or a bond-slip relationship as constitutive models since such data is easy to obtain from tests. However, in principle it is not important how the constitutive law for the interface material is defined since bond-slip or different softening shear moduli are just different ways of defining the same type of behavior. Ottosen & Olsson (1988) investigated the response of a symmetric, balanced double lap joint with linear hardening and softening using the same assumptions as in Volkersen (1938). Modeling of the adhesive was done traditionally using different shear modulus for the elastic and hardening/softening stiffness. Some important parameters describing the failure of a joint with softening behavior were identified, and design strategies were suggested.

This paper extends the solution by Volkersen and Ottosen & Olsson (1988) to include bi-linear softening. Focus is on calculation of the different stages a joint undergoes from first applied load to failure. The analysis results in explicit formulae for position of softening initiation at second softening branch, fracture initiation and load at different softening stages. The easy access to such important data and the ability to understand and investigate all parameters is

motivation for analyses like this, instead of studies performed with a finite element model. Examples are given in Section 4.

2 GOVERNING DIFFERENTIAL EQUATIONS

2.1 *Materials*

The outer adherents are marked with a subscript 1 and the inner adherent with 2. See
Figure 2a. They are both assumed linear elastic with Young's modulus E_1 and E_2. This results is the relations

$$\varepsilon_1(x) = \frac{\sigma_1(x)}{E_1} \tag{1}$$

$$\varepsilon_2(x) = \frac{\sigma_2(x)}{E_2} \tag{2}$$

where ε_1, σ_1 and ε_2, σ_1 denote the strain and stress in each adherent. The adhesive layer is described using a shear modulus G_x and a thickness t_a. The subscript of the shear modulus is dependent on the adhesive strain and is defined in the linear elastic stage as: G_e for $0 < \gamma \leq \gamma_{s1}$, first softening stage as: G_{s1} for $\gamma_{s1} < \gamma \leq \gamma_{s2}$ and second softening stage as: G_{s2} for $\gamma_{s2} < \gamma \leq \gamma_f$, where γ_{s1} and γ_{s2} denote the shear strain at softening initiation of stage one and two, and γ_f denotes the failure strain of the adhesive. The shear stress at onset of softening stage two is defined as τ_{s2}. See Figure1. 1.

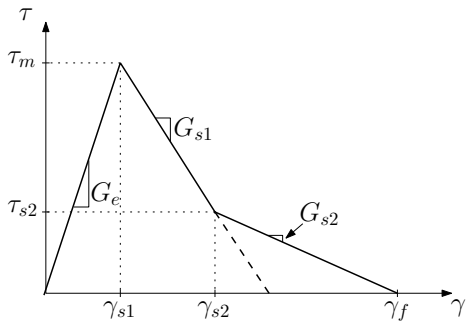

Figure 1. Constitutive relationship.

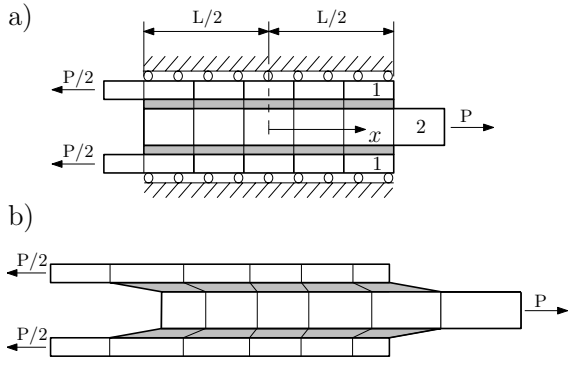

Figure 2. a) Geometry, definitions and boundary conditions for a double lap joint. b) Deformed shape of joint.

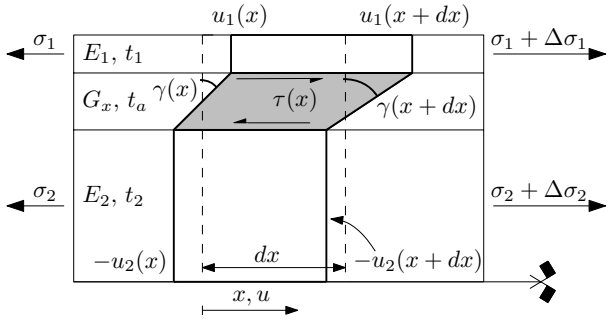

Figure 3. Equilibrium, deformation and materials in a joint.

The softening relationship is based upon a stress-slip relationship and formulated as a stress-strain relationship for convenience. This implies that the softening stress-strain relationship must be changed if the adhesive thickness is changed.

2.2 *Kinematic conditions*

The relationship between deformations and strain may be described when assuming small strains, by

$$\varepsilon_1(x) = \frac{du_1(x)}{dx} \tag{3}$$

$$\varepsilon_2(x) = \frac{du_2(x)}{dx} \tag{4}$$

$$\gamma(x) = \frac{1}{t_a}\left(u_2(x) - u_1(x)\right) \tag{5}$$

where the different parameters are defined in Figure 3. The adhesive layer is assumed to be loaded and deformed in pure shear.

2.3 *Equilibrium*

The horizontal equilibrium is obtained by summation of all forces acting in the infinitesimal element, see Figure 3. Note that only half the element is shown. Equilibrium provides:

$$t_1 \frac{d\sigma_1(x)}{dx} + \tau(x) = 0 \tag{6}$$

$$t_2 \frac{d\sigma_2(x)}{dx} - \tau(x) = 0 \tag{7}$$

Since the shear stress τ is related to the shear strain γ by $\tau(x) = \gamma(x)G_x$, we obtain by differentiation of this expression with respect to x and insertion of Equations (1)-(4).

$$\frac{d\tau(x)}{dx} = \frac{G_x}{t_a}\left[\frac{\sigma_2(x)}{E_2} - \frac{\sigma_1(x)}{E_1}\right] \tag{8}$$

Differentiation of (8) again and insertion of the equilibrium Equations (6) and (7) yields the differential equation

$$\frac{d^2\tau(x)}{dx^2} - \omega_x \tau = 0, \quad \omega_x = \frac{G_x}{t_a}\left[\frac{1}{E_1 t_1} + \frac{1}{E_2 t_2}\right], \quad \lambda_x = \sqrt{\omega_x} \tag{9}$$

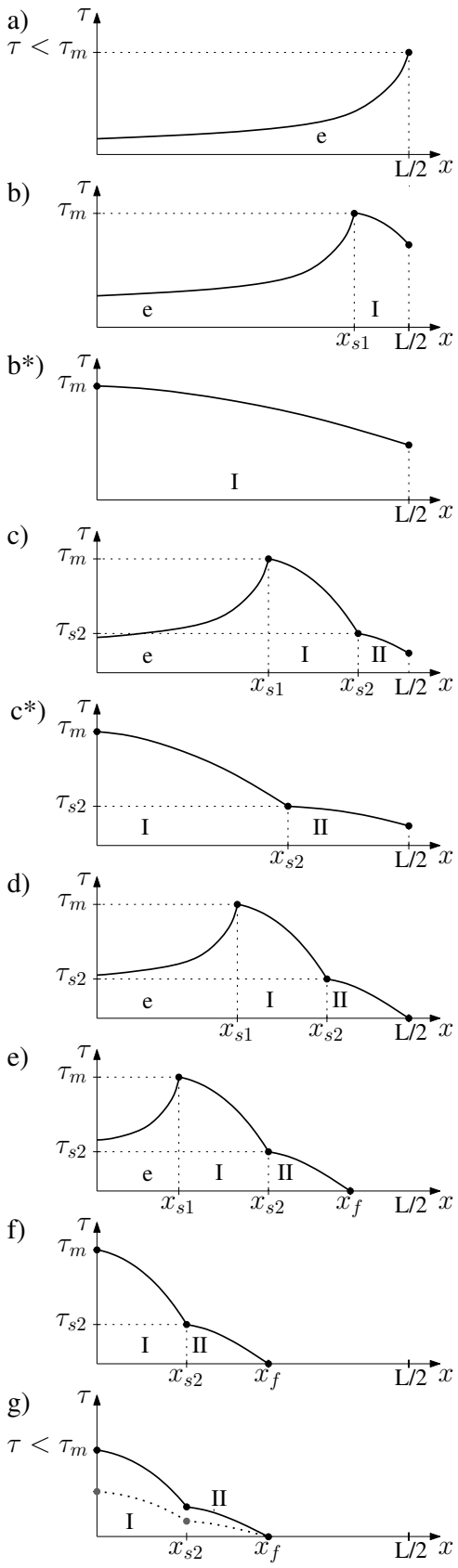

Figure 4. Schematic overview of the different stages a-g) during bi-linear softening of a balanced joint: a) Elastic, b) Elastic-softening(I), b*) Fully softening(I), c) Elastic-softening(I+II), c*) Fully softening(I+II), d) Onset of failure at Elastic-softening (I+II), e) Elastic-softening(I+II)-failure, f) Softening(I+II)–failure, g) Unloading.

At $x = -L/2$ it is known that $\sigma_1 = P/(2t_1 w)$ and $\sigma_2 = 0$, where t_1 is the thickness, w is the width of the joint and P is the applied force. Insertion in Equation (8) and applying the same method for $x = -L/2$ where $\sigma_2 = P/(2t_2 w)$ and $\sigma_1 = 0$ yields

$$\frac{d\tau}{dx} = -\frac{PG_x}{2t_a w E_1 t_1} \text{ for } x = -\frac{L}{2} \tag{10}$$

$$\frac{d\tau}{dx} = \frac{PG_x}{2t_a w E_2 t_2} \text{ for } x = \frac{L}{2} \tag{11}$$

Since we are analyzing a balanced symmetric joint, $E_1 t_1 = E_2 t_2$, Equation (12) holds and we define the useful constant Q_x.

$$\frac{d\tau}{dx} = Q_x = \frac{PG_x}{2t_a w E_1 t_1} = \frac{PG_x}{2t_a w E_2 t_2} \text{ for } x = \frac{L}{2} \tag{12}$$

In the forthcoming solutions we will only investigate positive x-values since the joint is symmetric.

3 JOINT ANALYSIS

The response of the joint is calculated by using appropriate boundary conditions and compatibility conditions. The solution scheme will closely follow the stages a-g) shown in Figure 4, and at the same time explain the stage in question.

3.1 *a) Elastic stage(e)*

In stage a) the shear stress in the joint has not yet reached the maximum shear stress, τ_m. The solution for the governing Equation (9) is then given in the interval $0 \le x \le L/2$ as

$$\tau(x) = C1\sinh(\lambda_e x) + C2\cosh(\lambda_e x) \tag{13}$$

Due to symmetry of the hyperbolic sine function, $C1=0$ and the following boundary condition is applied:

$$\frac{d\tau}{dx} = Q_e \text{ for } x = \frac{L}{2} \tag{14}$$

The solution yields

$$\tau(x) = \frac{Q_e \cosh(\lambda_e x)}{\lambda_e \sinh\left(\lambda_e \frac{L}{2}\right)} \tag{15}$$

The maximum force of this stage is obtained by setting $\tau(L/2) = \tau_m$ and applying the expression for Q_e, Equation (15). We obtain:

$$P_e = 2\frac{\tau_m}{G_e}\lambda_e t_a w E_1 t_1 \tanh\left(\lambda_e \frac{L}{2}\right) \quad (16)$$

w is the width of the joint.

3.2 *b) Elastic-softening(I)*

In stage b) the shear stress in the joint has reached the maximum shear stress, τ_m, at a point defined as x_{s1}. The solution for the governing Equation (9) is of the same type as (13). Using the same symmetry condition as in a) and applying the boundary condition

$$\tau(x_{s1}) = \tau_m \quad (17)$$

the response of the structure is given in the interval

$0 \leq x < xs_1$ as

$$\tau(x) = \frac{\tau_m \cosh(\lambda_e x)}{\cosh(\lambda_e x_{s1})} \quad (18)$$

The response in the interval $x_{s1} \leq x \leq L/2$ must be solved using differential Equation (9). The roots of the characteristic equation will be imaginary since G_{s1} and G_{s2} are negative. The solution is given as

$$\tau(x) = C3\sin(\lambda_x x) + C4\cos(\lambda_x x) \quad (19)$$

By applying boundary conditions

$$\tau(x = x_{s1}) = \tau_m \text{ and } \frac{d\tau}{dx} = Q_{s1}, \text{ for } x = L/2 \quad (20)$$

we obtain the solution

$$\tau(x) = \frac{\tau_m \lambda_{s1}\cos\left(\lambda_{s1}(L/2 - x)\right) + Q_{s1}\sin\left(\lambda_{s1}(x - x_{s1})\right)}{\lambda_{s1}\cos\left(\lambda_{s1}(L/2 - x_{s1})\right)} \quad (21)$$

This solution is valid until the shear stress reaches τ_{s2} at a distance $x = x_{s2}$, where the softening modulus changes. This distance can be found by iteration, demanding the expression in (21) equal to τ_{s2} and solving for x_{s2}

$$\tau_{s2} = \left[\tau_m \lambda_{s1}\cos\left(\lambda_{s1}\left(\frac{L}{2} - x_{s2}\right)\right) + Q_{s1}\sin\left(\lambda_{s1}(x_{s2} - x_{s1})\right)\right] \Big/ \lambda_{s1}\cos\left(\lambda_{s1}\left(\frac{L}{2} - x_{s1}\right)\right) \quad (22)$$

Q_{s1} is determined by applying a continuity condition at σ_1 and σ_2 for both the elastic and softening side of the solution in Equation (8). We obtain

$$\left[\frac{1}{G_e}\frac{d\tau}{dx}\right]_e = \left[\frac{1}{G_{s1}}\frac{d\tau}{dx}\right]_{s1}, \text{ for } x = x_{s1} \quad (23)$$

From this relationship, it is now possible to solve for Q_{s1}.

$$Q_{s1} = -\tau_m \lambda_{s1}\left[\frac{\lambda_{s1}}{\lambda_e}\cos\left(\lambda_{s1}(L/2 - x_{s1})\right)\tanh(\lambda_e x_{s1}) + \sin\left(\lambda_{s1}(L/2 - x_{s1})\right)\right] \quad (24)$$

where the relationship $G_e/G_{e1} = -\lambda_e^2/\lambda_{s1}^2$ has been used. The force is determined by Equation (12).

3.3 *b*) Softening(1)*

In stage b*) softening has reached $x_{s1} = 0$ before stage 2 softening has begun. This phenomenon is usually seen in very short joints, or joints with a soft adhesive. When the entire solution is defined to be in the softening region, the form of the solution is given in Equation (19). Using the same symmetry condition as in stage a) and applying the boundary condition

$$\frac{d\tau}{dx} = Q_{s1}, \text{ for } x = L/2 \quad (25)$$

the response of the structure in the interval $0 \leq x \leq L/2$ yields

$$\tau(x) = -\frac{Q_{s1}\cos(\lambda_{s1} x)}{\lambda_{s1}\sin\left(\lambda_{s1}\frac{L}{2}\right)} \quad (26)$$

3.4 *c) Elastic-softening(I+II)*

In stage c) the interval $0 \leq x < x_{s1}$ is still elastic and the solution in Equation (18) can be used.

The interval $x_{s1} \leq x < x_{s2}$, where x_{s2} was determined from Equation (22), softening is in stage 1. Boundary the following boundary conditions are applied to the general solution, Equation (19)

$$\tau(x = x_{s1}) = \tau_m \text{ and } \tau(x = x_{s2}) = \tau_{s2} \quad (27)$$

The solution yields

$$\tau(x) = \frac{\tau_{s2}\sin\left(\lambda_{s1}(x - x_{s1})\right) - \tau_m \sin\left(\lambda_{s1}(x - x_{s2})\right)}{\sin\left(\lambda_{s1}(x_{s2} - x_{s1})\right)} \quad (28)$$

The last interval $x_{s2} \leq x \leq L/2$ is in stage 2. This part of the solution is obtained by using the following boundary conditions in Equation (19)

$$\tau\left(x = x_{s2}\right) = \tau_{s2} \quad \text{and} \quad \frac{d\tau}{dx} = Q_{s2}, \ \text{for} \ x = L/2 \tag{29}$$

The response yields

$$\tau(x) = \frac{\tau_{s2}\lambda_{s2}\cos\left(\lambda_{s2}\left(L/2 - x\right)\right) + Q_{s2}\sin\left(\lambda_{s2}\left(x - x_{s2}\right)\right)}{\lambda_{s2}\cos\left(\lambda_{s2}\left(L/2 - x_{s2}\right)\right)} \tag{30}$$

To obtain the correct value for Q_{s2} and smooth transition between the two softening stages, the continuity between σ_1 and σ_2 in Equation (8) requires

$$\left[\frac{1}{G_{s1}}\frac{d\tau}{dx}\right]_{s1} = \left[\frac{1}{G_{s2}}\frac{d\tau}{dx}\right]_{s2}, \ \text{for} \ \ x = x_{s2} \tag{31}$$

Differentiating Equations (28) and (30), inserting into Equation (31) we obtain

$$\frac{Q_{s2}}{\lambda_{s2}\tau_{s2}\cos\left(\lambda_{s2}\left(x_{s2} - L/2\right)\right)} = \frac{\lambda_{s2}}{\lambda_{s1}}\left[\cot\left(\lambda_{s1}\left(x_{s2} - x_{s1}\right)\right) - \frac{\tau_m}{\tau_{s2}\sin\left(\lambda_{s1}\left(x_{s2} - x_{s1}\right)\right)}\right] + \tan\left(\lambda_{s2}\left(x_{s2} - L/2\right)\right) \tag{32}$$

Solving for Q_{s2} and using the relationship in Equation (12) to solve for the force P_{s2}, gives

$$P_{s2} = \frac{2t_a w E_1 t_1 Q_{s2}}{G_{s2}} \tag{33}$$

3.5 *c*) softening(I+II)*

In stage c*) $x_{s1} = 0$ and stage 2 softening has begun, but failure near $x = L/2$ is not initiated. The whole joint is thereby in the softening state.

The solution in the interval $0 \le x < x_{s2}$ may be calculated by applying symmetry leading to $C3 = 0$. The other boundary condition in Equation (19) is

$$\tau\left(x = x_{s2}\right) = \tau_{s2} \tag{34}$$

The solution yields

$$\tau(x) = \frac{\tau_{s2}\cos\left(\lambda_{s1}x\right)}{\cos\left(\lambda_{s1}x_{s2}\right)} \tag{35}$$

For $x_{s2} \le x \le L/2$ the solution in Equation (30) is still usable.

The maximum force in the joint can be obtained using Equation (32), setting $x_{s1} = 0$.

3.6 *d) Elastic-softening(I+II), onset of failure.*

The solution for Stage d) is identical to the one in Stage c). This stage is however interesting since failure and growth of a macro (stress-free) crack begins at $L/2$. Growth of the macro crack is described in Section 3.7.

The maximal load carried by the joint in this state is calculated by demanding $\tau(L/2) = 0$ in Equation (30). Reducing the expression and solving for Q_{s2} gives us:

$$Q_{s2} = -\frac{\tau_{s2}\lambda_{s2}}{\sin\left(\lambda_{s2}\left(L/2 - x_{s2}\right)\right)} \tag{36}$$

Applying Equation (12), the force in stage d) can be written as

$$P_d = -\frac{2t_a w E_1 t_1}{G_{s2}}\frac{\tau_{s2}\lambda_{s2}}{\sin\left(\lambda_{s2}\left(L/2 - x_{s2}\right)\right)} \tag{37}$$

To determine the maximal load at onset of failure, the distance x_{s2} corresponding to $\tau(L/2) = 0$, has to be known. The solution for this case is not directly available in closed form, and is therefore obtained by iteration. A simple iteration scheme can be setup as follows. If we equate Equation (30) to 0 at $L/2$, we obtain the following expression:

$$x_{s2} = \frac{L}{2} + \sin^{-1}\left(\frac{\tau_{s2}\lambda_{s2}}{Q_{s2}}\right)\frac{1}{\lambda_{s2}} \tag{38}$$

This equation is used along with Equation (36) to calculate expressions for x_{s2}, P_d and Q_{s2}. x_{s1} can be obtained from Equation (28) to plot the full response.

3.7 *e) Elastic-softening-failure*

The onset of the macro crack will start at $x = L/2$ when $\tau = 0$. A failed, stress free region will now start to grow from the end. The distance to this end is defined as x_f. This distance can be determined by first solving the differential equations, and secondly applying continuity conditions to parts of the solution.

One part of the joint is still elastic in the interval $0 \le x < x_{s1}$ and the solution in Equation (18) is still usable.

In the interval $x_{s1} \le x < x_{s2}$, where x_{s2} was determined from Equation (22), the response can still be determined by Equation (28).

Solution of the last interval $x_{s2} \le x \le x_f$ progresses as previously, where boundary conditions for solution of Equation (19) is

$$\tau\left(x = x_{s2}\right) = \tau_{s2} \quad \text{and} \quad \frac{d\tau}{dx} = Q_f, \ \text{for} \ x = x_f \tag{39}$$

Here Q_f is the first derivative of shear stress at x_f. The solution yields

$$\tau(x) = \frac{\tau_{s2}\lambda_{s2}\cos\left(\lambda_{s2}\left(x-x_f\right)\right)+Q_f\sin\left(\lambda_{s2}\left(x-x_{s2}\right)\right)}{\lambda_{s2}\cos\left(\lambda_{s2}\left(x_f-x_{s2}\right)\right)} \quad (40)$$

To find the distance x_f we must demand shear stress to be zero at x_f. Inserting $\tau(x_f) = 0$ in Equation (40) we obtain the expression for Q_f to be

$$Q_f = -\frac{\tau_{s2}\lambda_{s2}}{\sin\left(\lambda_{s2}\left(x_f-x_{s2}\right)\right)} \quad (41)$$

To obtain smooth transition between the two softening stages, the continuity between σ_1 and σ_2 in Equation (8) requires

$$\left[\frac{1}{G_{s1}}\frac{d\tau}{dx}\right]_{s1} = \left[\frac{1}{G_{s2}}\frac{d\tau}{dx}\right]_{s2}, \text{ for } x = x_{s2} \quad (42)$$

Differentiating Equations (28) and (40), inserting Q_f from Equation (41) and rearranging, yields

$$x_f = \cot^{-1}\left[\frac{\lambda_{s2}}{\lambda_{s1}}\left[\frac{\frac{\tau_m}{\tau_{s2}}-\cos\left(\lambda_{s1}\left(x_{s2}-x_{s1}\right)\right)}{\sin\left(\lambda_{s1}\left(x_{s2}-x_{s1}\right)\right)}\right]\right]\frac{1}{\lambda_{s2}}+x_{s2} \quad (43)$$

where $G_{s2}/G_{s1} = \lambda_{s2}^2/\lambda_{s1}^2$ has been used. The response in Equation (40) is then calculated at a value of x_{s1} by calculating x_f from Equation (43) followed by determination of Q_f from Equation (41). It is then possible to calculate the response. The force can be obtained by using relationship

$$Q_f = \frac{P_f G_{s2}}{2t_a w E_1 t_1}, \text{ for } x = x_f \quad (44)$$

or

$$P_f = -\frac{2t_a w E_1 t_1}{G_{s2}}\frac{\tau_{s2}\lambda_{s2}}{\sin\left(\lambda_{s2}\left(x_f-x_{s2}\right)\right)} \quad (45)$$

3.8 *f) softening(1+2)-failure*

In stage f), the distance x_{s1} has just reached zero and $\tau(0) = \tau_m$. In the interval $0 \le x < x_{s2}$ the response is determined from the same formula as in stage c*), Equation (35).

In the interval $x_{s2} \le x < x_f$, the solution from Equation (40) is still usable.

The force at full softening is obtained by setting $x_{s1} = 0$ in Equation (43) and using (45).

3.9 *g) Unloading*

In stage g) the softening region will remain constant and the load will decrease linearly. When the bearing capacity is completely exhausted, the softened region will fail, Ottosen & Olsson (1998). This has also been shown in Yuan et al. (2004). The principle is shown in Figure 4g with a dotted line. A fully correct analysis of the unloading response requires a definition of the unloading response in the constitutive relationship.

4 EXAMPLES

Two examples are given to illustrate some of the features and capabilities of this model. Some of these features are discussed in Section 5.

In the examples the slip is calculated at $L/2$ as

$$s(L/2) = \gamma(L/2)t_a \quad (46)$$

When a debonded, stress-free zone is present, the elastic elongation in adherent 1 must be added as

$$s(L/2) = \gamma(x_f)t_a + \frac{P}{E_1 t_1 w}\left(\frac{L}{2}-x_f\right) \quad (47)$$

4.1 *Moderate softening behavior*

Moderate softening behavior describes a joint where the absolute value of Gs1 does not differ much from Ge. Gs2 must not vary significantly from Gs1. The following constants have been chosen: L = 60; ta = 1; t1 = 2; t2 = t1; w = 1; E1 = 100000; E2 = E1; Ge = 30000; Gs1 = -20000; G_{s2}= -5000; τ_m = 5; τ_{s2} = 1.5.

Results are found in Figure 5 - Figure 6

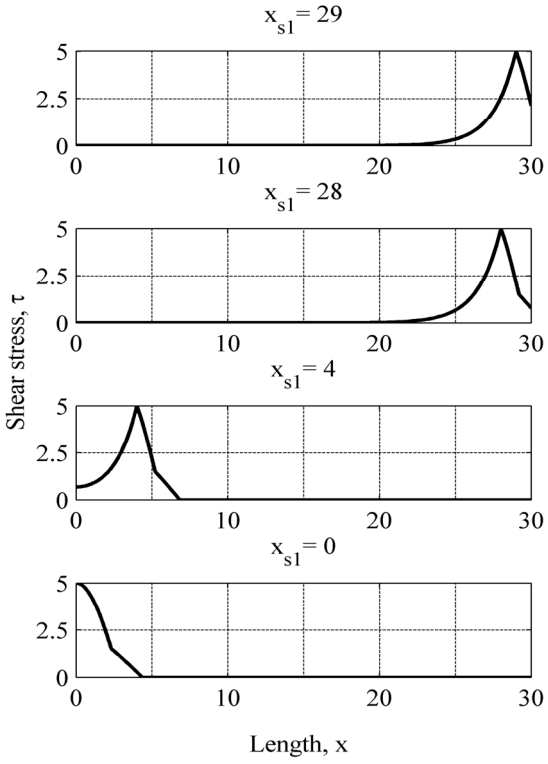

Figure 5. Shear stress distribution at different lengths of x_{s1}.

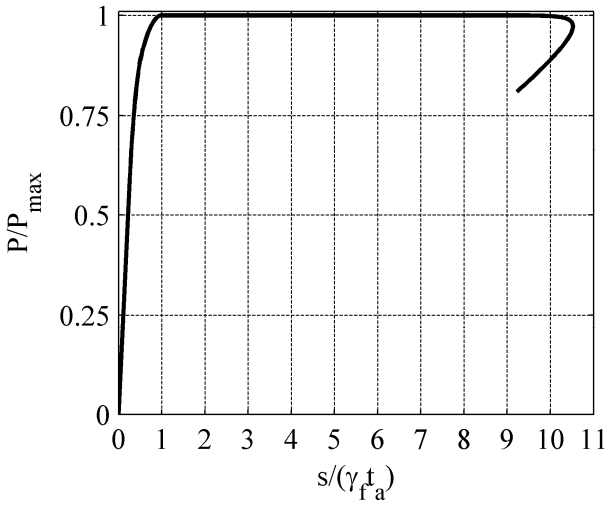

Figure 6. Relative load as a function of relative slip at $L/2$.

4.2 *Extreme softening behavior*

Extreme softening behavior is defined by softening branches where at least one has a near vertical or horizontal inclination. This example has the following constants: $L = 60$; $t_a = 1$; $t_1 = 2$; $t_2 = t_1$; $w = 1$; $E_1 = 100000$; $E_2 = E_1$; $G_e = 30000$; $G_{s1} = -100000$; $G_{s2} = -50$; $\tau_m = 5$; $\tau_{s2} = 0.75$.

Results are found in Figure 7 - Figure 8.

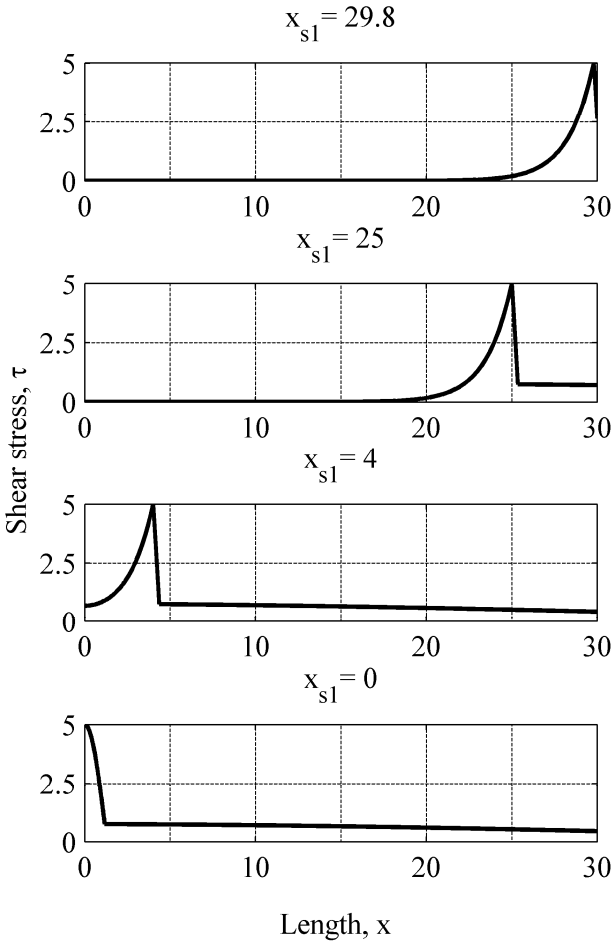

Figure 7. Shear stress distribution at different lengths of x_{s1}.

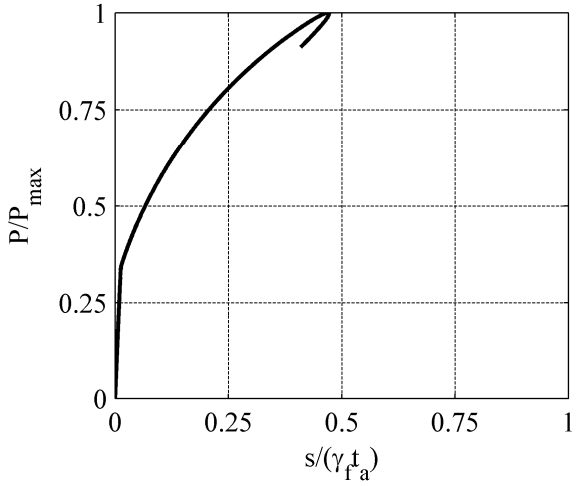

Figure 8. Relative load as a function of relative slip at $L/2$.

When values of x_{s1} approach 0 the values of x_f, may, in extreme cases, be seen to exhibit non-physical behavior, as it is the case with the current example. To obtain equilibrium in the solution, the combination of x_{s1}, x_{s2} and x_f is in Figure 9 seen to cause the onset of the stress-free crack to decrease. This is discussed further in Section 4.3 and 5.

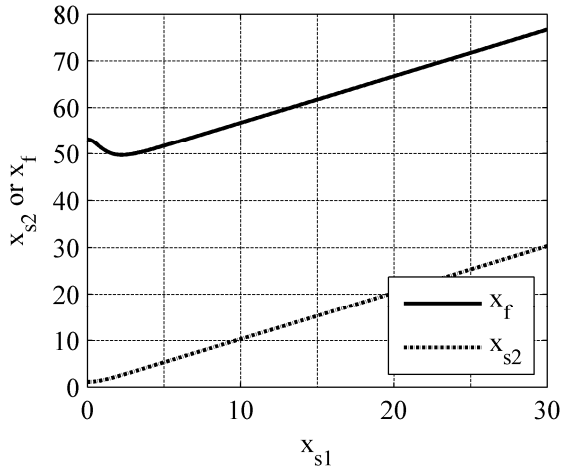

Figure 9. x_f and x_{s2} as a function of x_{s1}. Notice the special behavior of x_f for small values of x_{s1}.

4.3 *Parametric study, variation of G_{s2}*

A special observation was made when G_{s1} differed from G_{s2}. At some values of G_{s2}, the length of x_f would increase for decreasing values of x_{s1}. A phenomenon that is clearly non-physical, but nevertheless required by the solution. The behavior is shown in Figure 10. It is seen that x_f will behave as expected and obtain lowest value at $x_{s1} = 0$ from $G_{s2} \approx -20000$ and lower. $G_{s2} \approx -20000$ and higher, a peak error at around 4% on x_f is present.

Some variations on other parameters have shown to produce the same type of behavior. The subject is further discussed in Section 5. Material parameters for this case are: $L = 60$; $t_a = 1$; $t_1 = 2$; $t_2 = t_1$; $w = 1$;

E_1 = 100000; E_2 = E_1; G_e = 30000; G_{s1} = -30000; G_{s2}= -40000; τ_m = 5; τ_{s2} = 1.5.

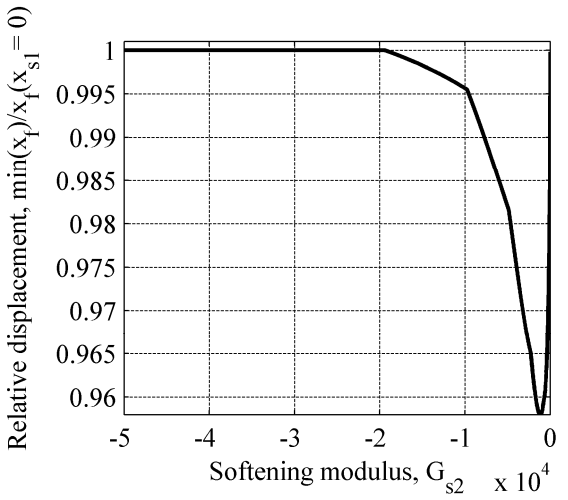

Figure 10. Relative displacement as a function of the second branch softening modulus, G_{s2}.

5 DISCUSSION AND CONCLUSION

A bi-linear softening curve to describe the behavior of the adhesive has been implemented in the solution for a tensioned adhesive joint in pure shear using well known assumptions. The joint was modeled after the classic Volkersen (1938) theory, which in other cases has proven to work well with tests. See for instance Yuan et al. (2004), and Täljsten (2008) where a theory based on Volkersen (1938) was used to evaluate the shear stress distribution in a strengthened steel plate.

The closed form solution of the proposed problem has proven capable of predicting the response for both moderate and extreme values of softening parameters. The moderate softening parameters resulted in a steady state delamination process with a almost constant fracturing load which ends up in a short unloading phase. Extreme softening parameters resulted in a peak-type load-slip response, followed by a short unloading phase. The failure shear strain was not reached in this case. A possible explanation for the load slip behavior might be found in Figure 9, where the onset of the stress-free crack is plotted. This point moves back through an already delaminated part of the crack at small values for x_{s1}, which is not physically possible. This may disturb the solution somewhat.

A parametric study showed a peculiar behavior of x_f when some parameters were varied. This is in particular the case with variations of the inclination of the second softening branch, G_{s2}. Results showed that the calculated distance to the debonded zone did not decrease for all values of x_{s1}, but instead increase near x_{s1} = 0. This solution is not physically allowable, but it is dictated by the equilibrium conditions and solution procedure. No final conclusions can be drawn from the initial study of this problem; however it is clear that the problem cannot be solved without a complete constitutive relationship for the adhesive describing the softening as well as the unloading behavior. A possibility for bypassing the problems caused by extreme softening parameters, is to derive the response of the joint as a function of displacement in an adherent; e.g. direct modeling of a deformation controlled test.

REFERENCES

Chen, J.F., Teng, J.G. 2001. Anchorage Strength Models for FRP and Steel Plates Bonded to Concrete. *Journal of Structural Engineering* 127(7):784-791.

Gustafsson, P.J. 1987. Analysis of generalized Volkersen-joints in terms of non-linear fracture mechanics. *Mechanical behavior of adhesive joints.* European mechanics colloquium 227. (Verchery, G. and Cardon, A.H.). 323-338.

Hart-Smith, L.J. 1973. Adhesive-bonded double-lap joints. *NASA-CR-112235.* Langley Research Center.

Ottosen, N.S. & Olsson, K.G., N. 1988., Hardening/Softening Plastic Analysis of Adhesive Joint. *Journal of Engineering Mechanics* 114(1):97-116.

Pichler, D. 1993. Die Virkung von Anpressungsdrücken auf die Verankerung von Klebelamellen(in German). Dissertation. *Universität Innsbruck.*

Ranisch, E-H. 1982. Zur Tragfähigkeit von Verkleberungen Zwischen Baustahl und Beton – Geklebte Bewehrung(in German). Dissertation. *TU Braunschweig.*

Täljsten, B. 1995. Strengthening of concrete prisms using the plate-bonding technique. *International Journal of Fracture.* 253-266.

Täljsten, B., Hansen, C.S., Schmidt, J.W. 2008. Strengthening of old metallic structures in fatigue with prestressed and non-prestressed CFRP laminates. *Construction and Building Materials.* 1665-1667.

Volkersen, O. 1938. Die Nietkraftverteilung in zugbeantspruchten Nietverbindungen mit konstanten Laschenquer-schnitten. *Luftfahrtforschung.* 15:41-47.

Yuan, H., Teng, J.G., Seracino, R., Wu, Z.S., Yao, J. 2004. Full range Behavior of FRP-to-concrete bonded joints. *Engineering Structures* 26:553-565.